



UNIVERSITY OF LEEDS

This is a repository copy of *The role of symmetry breaking in the structural trapping of light-induced excited spin states*.

White Rose Research Online URL for this paper:  
<http://eprints.whiterose.ac.uk/124591/>

Version: Accepted Version

---

**Article:**

Kulmaczewski, R [orcid.org/0000-0002-3855-4530](http://orcid.org/0000-0002-3855-4530), Trzop, E, Kershaw Cook, LJ et al. (3 more authors) (2017) The role of symmetry breaking in the structural trapping of light-induced excited spin states. *Chemical Communications*, 53 (99). pp. 13268-13271. ISSN 1359-7345

<https://doi.org/10.1039/C7CC07990G>

---

© 2017, The Royal Society of Chemistry. This is an author produced version of a paper published in *Chemical Communications*. Uploaded in accordance with the publisher's self-archiving policy.

**Reuse**

Items deposited in White Rose Research Online are protected by copyright, with all rights reserved unless indicated otherwise. They may be downloaded and/or printed for private study, or other acts as permitted by national copyright laws. The publisher or other rights holders may allow further reproduction and re-use of the full text version. This is indicated by the licence information on the White Rose Research Online record for the item.

**Takedown**

If you consider content in White Rose Research Online to be in breach of UK law, please notify us by emailing [eprints@whiterose.ac.uk](mailto:eprints@whiterose.ac.uk) including the URL of the record and the reason for the withdrawal request.



[eprints@whiterose.ac.uk](mailto:eprints@whiterose.ac.uk)  
<https://eprints.whiterose.ac.uk/>

# The Role of Symmetry Breaking in the Structural Trapping of Light-Induced Excited Spin States

Rafal Kulmaczewski<sup>a</sup>, Elzbieta Trzop<sup>b</sup>, Laurence J. Kershaw Cook<sup>c</sup>, Eric Collet<sup>\*b</sup>, Guillaume Chastanet<sup>\*d</sup> and Malcolm A. Halcrow<sup>\*a</sup>

**Light-Induced Excited Spin State Trapping (LIESST) data are reported for seven isostructural solvate salts from the iron(II)/2,6-di(pyrazol-1-yl)pyridine family. A complicated relationship between their spin-crossover  $T_{1/2}$  and  $T(\text{LIESST})$  values may reflect low-temperature thermal and light-induced symmetry breaking, which is shown by one of the compounds but not by two others.**

Spin-crossover (SCO) compounds<sup>1,2</sup> are versatile molecular switches for use in multifunctional materials, macroscopic devices and nanoscience.<sup>2,3</sup> SCO transitions can be induced by a range of stimuli including temperature, pressure and visible irradiation.<sup>1,4</sup> Light induced SCO is most often measured as a photo-conversion of a low-spin compound to a metastable high-spin state at low temperatures. This is the Light-Induced Excited Spin State Trapping (LIESST) effect.<sup>5</sup> The sample can only reconvert to its low-spin ground state upon heating above the activation barrier to its relaxation process, which typically lies below 150 K.

Mean-field theory of the propagation of SCO transitions through solid lattices predicts an inverse relationship between the thermodynamic SCO temperature  $T_{1/2}$  and the lifetime of the photoinduced metastable state,<sup>6</sup> Some years ago an empirical relationship of this type was indeed proposed in different families of compounds (eq 1):

$$T(\text{LIESST}) = T_0 - 0.3T_{1/2} \quad (1)$$

where  $T(\text{LIESST})$  is the relaxation temperature of the kinetically trapped spin state<sup>7,8</sup> and  $T_0$  reflects the rigidity of the metal ion coordination sphere.<sup>8,9</sup> Although there is often a degree of scatter in  $T_{1/2}$  vs  $T(\text{LIESST})$  plots, eq 1 is a useful predictor of  $T(\text{LIESST})$  for many types of SCO materials. This includes complex salts derived from  $[\text{Fe}(\text{bpp})_2]^{2+}$  ( $\text{bpp} = 2,6\text{-di}\{\text{pyrazol-1-yl}\}\text{pyridine}$ ), which often show good agreement to eq 1 with  $T_0 \approx 150$  K.<sup>10,11</sup>

<sup>a</sup> School of Chemistry, University of Leeds, Leeds LS2 9JT, UK. E-mail: m.a.halcrow@leeds.ac.uk

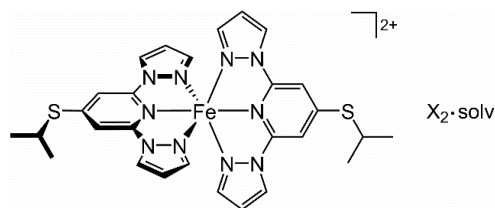
<sup>b</sup> Institut de Physique de Rennes, Université de Rennes 1, UMR UR1-CNRS 6251, F-35000 Rennes, France. E-mail: eric.collet@univ-rennes1.fr

<sup>c</sup> Department of Chemistry, University of Bath, Claverton Down, Bath BA2 7AY, UK.

<sup>d</sup> CNRS, Université de Bordeaux, ICMCB, UPR 9048, F-33600 Pessac, France. E-mail: chastanet@icmcb-bordeaux.cnrs.fr

† Electronic Supplementary Information (ESI) available: experimental procedures and characterisation data; crystallographic experimental data, Figures and Tables; magnetic susceptibility data for all the compounds, measured under the same conditions as in ref. 12; kinetic studies of thermal SCO in two  $1[\text{ClO}_4]_2\cdot\text{solv}$  samples; and a Table of the  $T(\text{LIESST})$  data plotted in Fig. 2. See DOI: 10.1039/x0xx00000x

We recently reported six compounds of general formula  $[\text{Fe}L_2][\text{BF}_4]_2\cdot\text{solv}$  ( $1[\text{BF}_4]_2\cdot\text{solv}$ , Scheme 1).<sup>12</sup> This is a rare family of isostructural SCO materials,<sup>13</sup> which facilitates studies of structure: function relationships underlying their SCO behaviour. We have expanded the series with the perchlorate salts  $1[\text{ClO}_4]_2\cdot\text{solv}$ , and report a photomagnetic and photocrystallographic study on these isostructural compounds that reveals the relationship between structure and  $T(\text{LIESST})$  in unprecedented detail.



**Scheme 1.** Compound  $1X_2\cdot\text{solv}$  ( $X^- = \text{BF}_4^-$  or  $\text{ClO}_4^-$ ;  $\text{solv} = \text{MeNO}_2, \text{MeCN}, \text{Me}_2\text{CO}, \text{H}_2\text{O}$  or  $\text{sf}$  [solvent-free]).

Complexation of  $\text{Fe}[\text{ClO}_4]_2\cdot 6\text{H}_2\text{O}$  by 2 equiv  $L$  in the appropriate solvent affords  $1[\text{ClO}_4]_2\cdot\text{MeCN}$ ,  $1[\text{ClO}_4]_2\cdot\text{MeNO}_2$  and  $1[\text{ClO}_4]_2\cdot y\text{Me}_2\text{CO}$  ( $y \approx 0.7$ ) after the usual work-up.  $1[\text{ClO}_4]_2\cdot y\text{Me}_2\text{CO}$  is converted to  $1[\text{ClO}_4]_2\cdot\text{H}_2\text{O}$  in single-crystal-to-single-crystal fashion, when stored *in vacuo* at 290 K for 24 hrs and then exposed to air. Solvent-free  $1[\text{ClO}_4]_2\cdot\text{sf}$  was also prepared *in situ*, by annealing crystals of  $1[\text{ClO}_4]_2\cdot y\text{Me}_2\text{CO}$  on the diffractometer (ESI †). The  $1[\text{ClO}_4]_2\cdot\text{solv}$  and  $1[\text{BF}_4]_2\cdot\text{solv}$ <sup>12</sup> compounds are high-spin, isostructural and phase-pure at room temperature ( $P2_1/c$ ,  $Z = 4$ ), while all except  $1[\text{ClO}_4]_2\cdot\text{MeCN}$  exhibit SCO upon cooling without a crystallographic phase change (Fig. 1 and ESI †). The SCO temperature and cooperativity vary between the compounds, but the high-spin state is consistently stabilised when  $X = \text{ClO}_4^-$  compared to  $X = \text{BF}_4^-$  for each solvent. That might reflect expansion of the crystal lattice by the larger  $\text{ClO}_4^-$  anion, which would favour the larger high-spin cations.<sup>14</sup> Any fraction of the samples that is high-spin near 100 K remains frozen in below that temperature.<sup>15,16</sup> Poising  $1[\text{ClO}_4]_2\cdot\text{MeNO}_2$  at 102 K for 80 mins leads to a slow reduction in  $\chi_M T$ , until the sample is fully low-spin and the warming branch of the transition proceeds monotonically (ESI †). That confirms the kinetic origin of the low-temperature spin-state trapping, and the apparent SCO hysteresis, in that material. Such kinetic effects arise when thermal trapping of the high-spin state occurs at a similar temperature to  $T_{1/2}$  in an SCO material.<sup>15</sup>

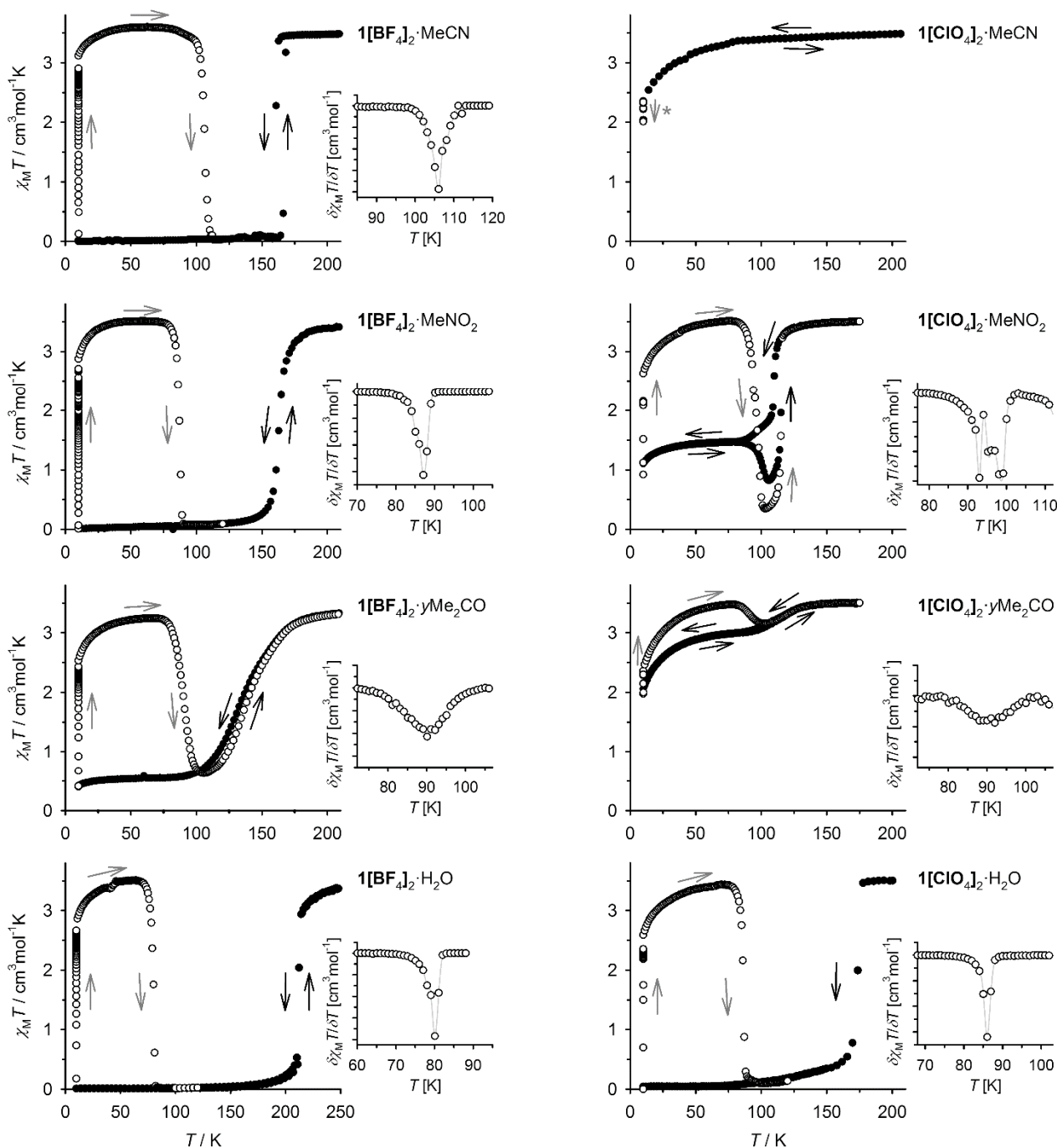


**Figure 1.** Temperature dependence of magnetic susceptibility data for eight  $1\mathbf{X}_2$ -solv compounds before irradiation ( $\bullet$ , black arrows), and during the  $T(\text{LIESST})$  measurement ( $\circ$ , grey arrows). The samples were cooled to 10 K, irradiated at that temperature ( $\lambda = 510$  nm), then rewarmed in the dark. Scan rate  $0.4 \text{ Kmin}^{-1}$ . The insets show the first derivatives of the relaxation curves, with data points linked by spline curves for clarity. The starred compound is high-spin at 10 K, and was irradiated at  $\lambda = 980$  nm in a reverse-LIESST experiment.<sup>17</sup>

Seven freshly prepared  $1\mathbf{X}_2$ -solv samples showed essentially quantitative low $\rightarrow$ high-spin photoconversion upon irradiation at 510 nm at 10 K (Fig. 1). After equilibration, warming the samples in the dark showed the high-spin forms are long-lived until ca 80 K, where thermal relaxation to their thermodynamic low-spin states took place.<sup>17</sup> The  $T(\text{LIESST})$  curves are mostly monotonic but of differing abruptness, with samples exhibiting the least cooperative thermal SCO ( $1[\text{BF}_4]_2 \cdot y\text{Me}_2\text{CO}$  and  $1[\text{ClO}_4]_2 \cdot y\text{Me}_2\text{CO}$ ) showing the most gradual LIESST relaxation. An exception is  $1[\text{ClO}_4]_2 \cdot \text{MeNO}_2$ , whose relaxation is split into three closely spaced components.

Although other explanations are possible,<sup>18</sup> this stepped relaxation may reflect crystallographic phase changes occurring during the LIESST relaxation process (see below).<sup>19</sup>

The  $T(\text{LIESST})$  values, from the minima of the  $\delta\chi_M T / \delta T$  curves, are typical for complexes of this type (Table 1).<sup>11</sup> However, a plot of  $T_{1/2}$  vs  $T(\text{LIESST})$  for these data can be interpreted in two ways (Fig. 2). At first glance, all the compounds lie on the same  $T(\text{LIESST})/T_{1/2}$  line except  $1[\text{BF}_4]_2 \cdot \text{MeCN}$ , whose  $T(\text{LIESST})$  is ca 20 K higher than for  $1[\text{BF}_4]_2 \cdot \text{MeNO}_2$  despite their similar  $T_{1/2}$  values (Table 1). However, comparison of these data with the literature shows an



**Table 1.** Thermal SCO and LIESST properties of  $1[\text{BF}_4]_2\text{-solv}$  and  $1[\text{ClO}_4]_2\text{-solv}$ , with a temperature ramp of  $0.4\text{ Kmin}^{-1}$ . (Figs. 1 and 2). Data for the  $\text{BF}_4^-$  salts differ slightly from those in ref. 13, which were measured at a faster scan rate of  $5\text{ Kmin}^{-1}$  (ESI †).

	$T_{1/2}\downarrow / \text{K}$	$T_{1/2}\uparrow / \text{K}$	cooperativity	$T(\text{LIESST}) / \text{K}$
$1[\text{BF}_4]_2\text{-MeCN}$	160	167	abrupt	106
$1[\text{ClO}_4]_2\text{-MeCN}$	HS <sup>a</sup>	–	–	–
$1[\text{BF}_4]_2\text{-MeNO}_2$	171	–	gradual	87
$1[\text{ClO}_4]_2\text{-MeNO}_2$	102	115	gradual, incomplete	93,96,99
$1[\text{BF}_4]_2\cdot\gamma\text{Me}_2\text{CO}$	131	–	gradual, incomplete	91
$1[\text{ClO}_4]_2\cdot\gamma\text{Me}_2\text{CO}$	<100 <sup>b</sup>	–	gradual, incomplete	ca 90 <sup>c</sup>
$1[\text{BF}_4]_2\cdot\text{H}_2\text{O}$	212	214	abrupt	81
$1[\text{ClO}_4]_2\cdot\text{H}_2\text{O}$	173	–	abrupt	86

<sup>a</sup>HS = high-spin between 3-300 K. <sup>b</sup>Only 20 % of the SCO transition occurs before the remaining high-spin fraction is frozen in below 100 K. <sup>c</sup>Not included in Fig. 2.

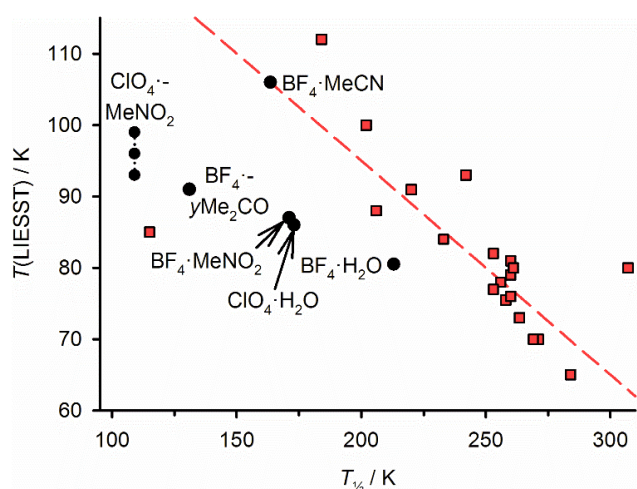


**Figure 2.** Plot of  $T_{1/2}$  vs  $T(\text{LIESST})$  for the compounds in this work (black circles; Table 1), and from previously published compounds from our laboratory (red squares; ESI†). The dashed line shows eq 1 with  $T_0 = 155\text{ K}$ , close to the  $T_0 = 150\text{ K}$  correlation that was originally proposed for this family of compounds.<sup>10,11</sup>

alternative picture. Only  $1[\text{BF}_4]_2\text{-MeCN}$  and  $1[\text{BF}_4]_2\text{-H}_2\text{O}$  lie within experimental error of the trend expected from our previous measurements. The other compounds show reduced  $T(\text{LIESST})$  values, deviating increasingly from eq 1 as  $T_{1/2}$  is lowered (Fig. 2). Crystallographic studies on three of the materials shed light on these differences. Unexpectedly,  $1[\text{BF}_4]_2\text{-MeNO}_2$  undergoes a symmetry-breaking phase transition upon cooling from 100 K (phase 1;  $P2_1/c$ ,  $Z = 4$ ) to 15 K (phase 2;  $P2_1/c$ ,  $Z = 12$ ), involving a tripling of the unit cell  $b$  dimension. Three unique low-spin cations in the asymmetric unit, labelled ‘A’, ‘B’ and ‘C’, are grouped into layers parallel to (010). Individual layers contain either A-type molecules or alternating B and C types, with the layers arranged as A–(B/C)–(B/C)–A–(B/C)–(B/C) down the  $b$  axis (Fig. 3). Irradiation at 660 nm at 15 K transforms the crystal to a new high-spin phase (phase 3;  $P2_1$ ,  $Z = 4$ ), whose unit cell dimensions resemble phase 1 but which lacks the  $c$  glide plane. The ‘A’ and ‘B’ cation sites in this phase are grouped into corrugated layers along (001) (Fig. 4). The cations in phases 2 and 3 have similar metric parameters to the corresponding spin states of phase 1. The symmetry breaking is reflected in changes to the orientations of the *isopropyl* groups, anions and solvent molecules (ESI †).

In contrast,  $1[\text{BF}_4]_2\text{-H}_2\text{O}$  (at 20 K) and  $1[\text{BF}_4]_2\text{-MeCN}$  (at 85 K) both retain phase 1 before and after irradiation; the high-spin form

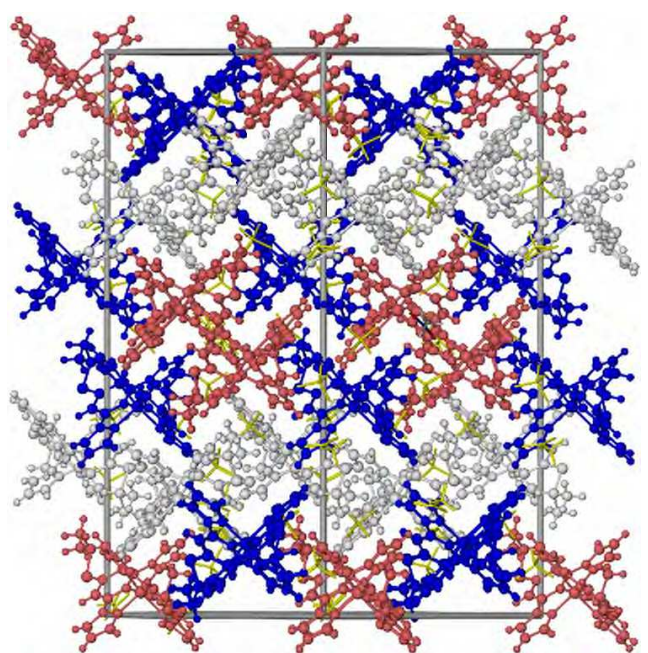


**Figure 3.** Packing diagram of low-spin phase 2 of  $1[\text{BF}_4]_2\text{-MeNO}_2$  along the (101) crystal vector, with the  $b$  axis vertical. Cations A, B and C are coloured white, blue and red, respectively, while the anions and solvent (yellow) are de-emphasised for clarity.

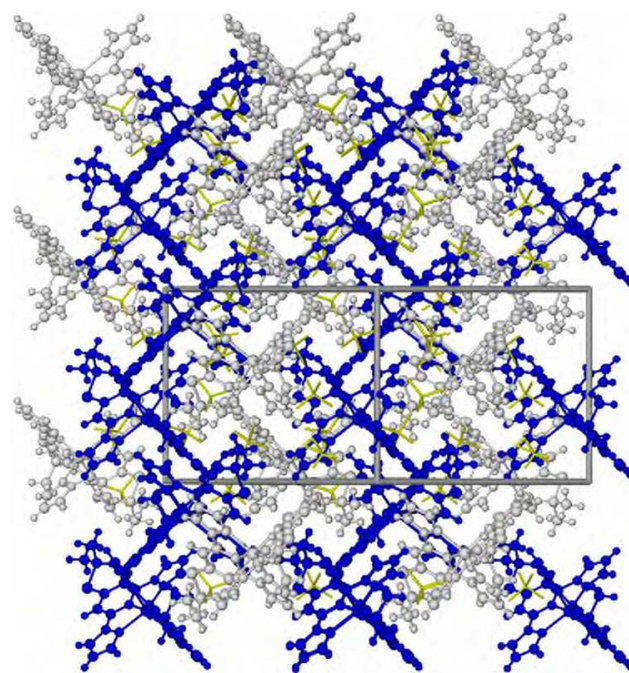


**Figure 4.** Packing diagram of high-spin phase 3 of  $1[\text{BF}_4]_2\text{-MeNO}_2$ , in the same view as Fig. 3. Cations A and B are coloured white and blue, respectively. Other details as for Fig. 3.

of  $1[\text{BF}_4]_2\text{-MeCN}$  was also characterised at 15 K, again adopting phase 1. Hence  $1[\text{BF}_4]_2\text{-H}_2\text{O}$  and  $1[\text{BF}_4]_2\text{-MeCN}$ , which align more closely with eq 1 ( $T_0 = 150\text{ K}$ , Fig. 2), show no evidence for symmetry breaking under these conditions. The isothermal low-spin→high-spin photoconversion of both phase 1 compounds results in an expansion of the unit cell  $a$  axis and a contraction of  $b$  and  $\beta$ . The reduction in  $\beta$  is much larger for  $1[\text{BF}_4]_2\text{-MeCN}$  at 85 K, causing an unusual 0.2 % contraction of the unit cell volume in its

high-spin state. In contrast,  $1[\text{BF}_4]_2 \cdot \text{H}_2\text{O}$  and  $1[\text{BF}_4]_2 \cdot \text{MeNO}_2$  both undergo a more typical expansion of their normalised unit cell volume during photoexcitation experiments (ESI †).

The light-induced high-spin state of  $1[\text{BF}_4]_2 \cdot \text{MeNO}_2$  (phase 3) has reduced crystallographic symmetry, and thus a lower entropy, than its thermodynamic high-spin state (phase 1). That should shift the (theoretical)  $T_{1/2}$  of phase 3 to a higher temperature than phase 1,<sup>20</sup> leading to a lower  $T(\text{LIESST})$  for phase 3 as observed (eq 1).<sup>21</sup> This symmetry-breaking entropy change is unlikely to be electronic in origin, since the coordination geometries of the  $C_1$ -symmetric iron centers are similar in each phase. Rather, it predominantly reflects a reduction in vibrational entropy through a lifting of lattice phonon degeneracy, associated with the loss of the crystallographic glide plane and inversion center in phase 3. Attempts to access phase 1 of  $1[\text{BF}_4]_2 \cdot \text{MeNO}_2$  by photoirradiation, for comparison with phase 3, have thus far been unsuccessful.

In conclusion, isostructural  $1[\text{BF}_4]_2 \cdot \text{solv}$  and  $1[\text{ClO}_4]_2 \cdot \text{solv}$  exhibit a complex relationship between  $T_{1/2}$  and  $T(\text{LIESST})$ . Most of the compounds exhibit a linear  $T_{1/2}$  vs  $T(\text{LIESST})$  dependence, with a reduced slope compared to eq 1 (Fig. 2). Hence, a generalisation of eq 1 can be applied to this subset of compounds (eq 2).

$$T(\text{LIESST}) = T_0 - aT_{1/2} \quad (2)$$

The data in Table 1 (omitting  $1[\text{BF}_4]_2 \cdot \text{MeCN}$ ) are best fit by  $T_0 = 108 \text{ K}$  and  $a = 0.13$  (ESI †). Moreover,  $T(\text{LIESST})$  for  $1[\text{BF}_4]_2 \cdot \text{MeCN}$  and  $1[\text{BF}_4]_2 \cdot \text{MeNO}_2$  differ by 20 K, despite their almost identical  $T_{1/2}$  values (Table 1). That can be explained by the thermodynamic consequences of a series of thermal and light-induced symmetry-breaking transitions, which are undergone by  $1[\text{BF}_4]_2 \cdot \text{MeNO}_2$  but not  $1[\text{BF}_4]_2 \cdot \text{MeCN}$  or  $1[\text{BF}_4]_2 \cdot \text{H}_2\text{O}$ . This clearly demonstrates the impact of crystallographic phase changes on  $T(\text{LIESST})$ ,<sup>21</sup> at least in these two compounds. Other compounds that deviate unexpectedly from eqs 1 or 2 may also exhibit unresolved structural chemistry in the LIESST experiment.

This work was funded by EPSRC grants EP/K012568/1 and EP/K012576/1; and by the National Research Agency (ANR-13-BS04-0002), Rennes Metropole and CNRS. The Aquitaine Region is acknowledged for the development of the International Centre of Photomagnetism in Aquitaine (ICPA) platform. Support by COST network CM1305 *Explicit Control of Spin States in Technology and Biology (ECOSTBio)* is also acknowledged. Data supporting this study are available at <http://doi.org/10.5518/292>.

## Conflicts of interest

There are no conflicts to declare.

## Notes and references

- 1 *Spin-crossover materials - properties and applications*, ed. M. A. Halcrow, John Wiley & Sons, Chichester, 2013, p. 568.
- 2 K. S. Kumar and M. Ruben, *Coord. Chem. Rev.*, 2017, **346**, 176.
- 3 M. D. Manrique-Juárez, S. Rat, L. Salmon, G. Molnár, C. M. Quintero, L. Nicu, H. J. Shepherd and A. Bousseksou, *Coord. Chem. Rev.*, 2016, **308**, 395.
- 4 P. Guionneau, *Dalton Trans.*, 2014, **43**, 382; R. Bertoni, M. Lorenc, A. Tissot, M.-L. Boillot and E. Collet, *Coord. Chem. Rev.*, 2015, **282–283**, 66.
- 5 S. Decurtins, P. Gutlich, C. P. Köhler, H. Spiering and A. Hauser, *Chem. Phys. Lett.*, 1984, **105**, 1.
- 6 A. Hauser, J. Jeftić, H. Romstedt, R. Hinek and H. Spiering, *Coord. Chem. Rev.*, 1999, **190–192**, 471.
- 7 J.-F. Létard, L. Capes, G. Chastanet, N. Moliner, S. Létard, J. A. Real and O. Kahn, *Chem. Phys. Lett.*, 1999, **313**, 115.
- 8 J.-F. Létard, *J. Mater. Chem.*, 2006, **16**, 2550.
- 9 J.-F. Létard, G. Chastanet, P. Guionneau and C. Desplanches in *Spin-crossover materials – properties and applications*, ed. M. A. Halcrow, John Wiley & Sons, Chichester, UK, 2013, ch. 19, p. 475–506.
- 10 S. Marcen, L. Lecren, L. Capes, H. A. Goodwin and J.-F. Létard, *Chem. Phys. Lett.*, 2002, **358**, 87.
- 11 M. A. Halcrow, *Coord. Chem. Rev.*, 2009, **253**, 2493.
- 12 L. J. Kershaw Cook, R. Kulmaczewski, O. Cespedes and M. A. Halcrow, *Chem. Eur. J.*, 2016, **22**, 1789.
- 13 See eg M. Hostettler, K. W. Törnroos, D. Chernyshov, B. Vangdal and H.-B. Bürgi, *Angew. Chem., Int. Ed.*, 2004, **43**, 4589; M. Yamada, H. Hagiwara, H. Torigoe, N. Matsumoto, M. Kojima, F. Dahan, J.-P. Tuchagues, N. Re and S. Iijima, *Chem. Eur. J.*, 2006, **12**, 4536; R. Pritchard, C. A. Kilner and M. A. Halcrow, *Chem. Commun.*, 2007, 577; T. Sato, K. Nishi, S. Iijima, M. Kojima and N. Matsumoto, *Inorg. Chem.*, 2009, **48**, 7211; R.-J. Wei, J. Tao, R.-B. Huang and L.-S. Zheng, *Inorg. Chem.*, 2011, **50**, 8553.
- 14 The unit cell volume of  $1\text{X}_2 \cdot \text{solv}$  at 250 K is 1.0–2.0 % larger when  $\text{X} = \text{ClO}_4^-$  than for  $\text{X} = \text{BF}_4^-$ , for each solvent. The anion, solvent and *isopropyl* group disorder in  $1[\text{BF}_4]_2 \cdot \text{solv}$  and  $1[\text{ClO}_4]_2 \cdot \text{solv}$ , for any given solvent, is essentially identical in each spin state (ESI †).<sup>12</sup> Hence,  $T_{1/2}$  is less likely to be influenced by crystallographic disorder in the different salts.
- 15 See eg G. Ritter, E. König, W. Irlner and H. A. Goodwin, *Inorg. Chem.*, 1978, **17**, 204; V. A. Money, C. Carbonera, J. Elhaik, M. A. Halcrow, J. A. K. Howard and J.-F. Létard, *Chem. Eur. J.*, 2007, **13**, 5503; J.-F. Létard, S. Asthana, H. J. Shepherd, P. Guionneau, A. E. Goeta, N. Suemura, R. Ishikawa and S. Kaizaki, *Chem. Eur. J.*, 2012, **18**, 5924.
- 16 G. A. Craig, J. S. Costa, S. J. Teat, O. Roubeau, D. S. Yufit, J. A. K. Howard and G. Aromí, *Inorg. Chem.*, 2013, **52**, 7203.
- 17 A reverse-LIESST<sup>8,9</sup> experiment was also attempted on high-spin  $1[\text{ClO}_4]_2 \cdot \text{MeCN}$ . No high→low-spin photoconversion was observed at 830 or 980 nm, however (Fig. 1).
- 18 V. Niel, A. L. Thompson, A. E. Goeta, C. Enachescu, A. Hauser, A. Galet, M. C. Muñoz and J. A. Real, *Chem. Eur. J.*, 2005, **11**, 2047; P. Chakraborty, C. Enachescu and A. Hauser, *Eur. J. Inorg. Chem.*, 2013, 770.
- 19 S. Pillet, E. Bendeif, S. Bonnet, H. J. Shepherd and P. Guionneau, *Phys. Rev. B*, 2012, **86**, 064106; K. D. Murnaghan, C. Carbonera, L. Toupet, M. Griffin, M. M. Dîrtu, C. Desplanches, Y. Garcia, E. Collet, J.-F. Létard and G. G. Morgan, *Chem. Eur. J.*, 2014, **20**, 5613; H. Watanabe, K. Tanaka, N. Bréfuel, H. Cailleau, J.-F. Létard, S. Ravy, P. Fertey, M. Nishino, S. Miyashita and E. Collet, *Phys. Rev. B*, 2016, **93**, 014419.
- 20 T. Tayagaki and K. Tanaka, *Phys. Rev. Lett.*, 2001, **86**, 2886.
- 21 A. L. Thompson, A. E. Goeta, J. A. Real, A. Galet and M. C. Muñoz, *Chem. Commun.*, 2004, 1390.